

# Dynamic Behavior of Thousand-meter Scale Cable-stayed Bridge with Hybrid FRP Cables

ハイブリッドFRPケーブルによる1000メートル尺的な斜張橋の動的挙動

Xin WANG\* and Zhishen WU\*\*

汪昕・吳智深

\*PhD Candidate Dept. of Urban and Civil Eng., Ibaraki University (Nakanarusawa-cho 4-12-1, Hitachi, 316-8511)

\*\* Member Dr. of Eng. Prof. Dept. of Urban and Civil Eng., Ibaraki University (Nakanarusawa-cho 4-12-1, Hitachi, 316-8511)

This paper investigates a new type of hybrid fiber-reinforced polymer (FRP) cable applied in thousand-meter scale cable-stayed bridge with a special emphasis on the dynamic behavior of the bridges and cables. The limitations of conventional steel stay cables and the advantages of hybrid basalt and carbon FRP (B/CFRP) cables were first clarified, in terms of which the dynamic behavior of cable-stayed bridges that has two main spans (1088m and 2176m) with steel, carbon, basalt and hybrid B/CFRP cables were analyzed respectively by means of finite element method. Results show that the hybrid B/CFRP cable compared with the steel cables exhibits much higher natural frequencies, which could lower the possibility of resonance induced by interaction between stay cables and the bridge. Furthermore, the aerodynamic stability of hybrid B/CFRP cables may be superior to the other cables due to its adjustable inherent damping.

**Key Words:** *dynamic behavior, hybrid FRP, thousand-meter scale, cable-stayed bridge*

## 1. Introduction

The application of cable-stayed bridges to cross wide rivers or sea bays has developed rapidly in the past thirty years, and they have become a widely used type of long-span bridges, due to the superior self-balancing structural system, higher overall stiffness and better aerodynamic behavior in comparison to suspension bridges<sup>1)</sup>. Currently, the three longest cable-stayed bridges around the world are Sutong Bridge (1,088 m) in China, Stonecutters Bridge (1,018 m, expected to be completed in 2009) in Hong Kong China, and Tatara Bridge (890m) in Japan respectively. Cable-stayed bridges have already reached the thousand-meter scale that was previously the economical span only for suspension bridges. Moreover, even longer spans have been planned<sup>2-3)</sup>.

However, for cable-stayed bridges with a span of thousand-meter scale, traditional materials, such as steel cables, and concrete or steel main girders, may restrict their advantages because of their significantly increased weight with elongation of span and relatively poor durability. Some researchers have investigated cable materials, static and dynamic factors that limit

the elongation of main spans<sup>4-5)</sup>. For instance, for steel cables, the equivalent modulus induced by the sag effect will decrease obviously with the elongation of the main span, which results in a weakening of the entire bridge stiffness, making the structure more flexible. This phenomenon is primarily caused by the high density of steel cable. In addition, the degradation of steel cables seriously affects the safety and durability of bridges. Although some treatments may be used to protect steel cables from environmental degradation, corrosion still easily occurs at the anchorage zones due to the damage caused by frequent vibration. Therefore, to solve above problems, a new type of cable with high strength, light weight and superior durability should be developed to achieve both short-term and long-term superior performance for thousand-meter scale cable-stayed bridge.

In the past twenty years, the applications of fiber-reinforced polymer (FRP) materials have been greatly developed in civil engineering. Besides retrofitting and strengthening existing structures, FRP materials are gradually being applied more often in new structures, including FRP bridge decks, FRP bars in concrete structures and FRP hybrid beams and columns<sup>6-8)</sup>, because of their superior mechanical and chemical properties,

such as the high strength-to-weight ratio, anti-corrosion properties, fatigue-resistance and ease of tailoring. Applications of FRP materials in super-long span bridges have been discussed worldwide for many years, among which the most famous one is the 8,400 m span cable-stayed bridge with CFRP cables across the Strait of Gibraltar proposed by Meier<sup>2)</sup>. The structural system, cost comparison and feasibility were discussed in detail for this bridge. After that, many investigations and experiments have been conducted regarding applications of FRP cables<sup>9)</sup>, especially for the anchorage<sup>10-11)</sup>. Meanwhile, some pedestrian and vehicular bridges have been constructed for the purpose of testing the real performance of FRP cables, such as Aberfeldy footbridge (UK, 1992), Herning bridge (Denmark, 1999), I-5/Gilman bridge (USA, 2002)<sup>12)</sup>, and a pedestrian bridge at Jiangsu Univ. (China, 2004)<sup>4)</sup>.

In previous studies of composite cable-stayed bridges, carbon fiber composites are applied as stay cables to overcome the shortcomings of steel cables due to their better mechanical and chemical properties than other fiber composites such as glass or aramid fibers. However, the high and continually increasing cost of carbon fibers restricts their development and applications in new structures, especially in large-scale construction like bridges or spatial structures. Additionally, the sensitivity of CFRP cables to the wind load is difficult to control due to their extremely light weight and high strength. In these cases, an economical fiber composite with integrated high performance would be necessary for stay cables. Glass fiber composite was initially considered due to their wide utilization in civil infrastructures for many years, combined with their low cost and high strength compared to traditional materials. However, their low fatigue strength, large creep and poor durability (i.e., sensitivity to alkali effects) may cause inferior long-term performance and durability problems. Aramid fiber composite also has a problem of high cost; furthermore their modulus is much lower in comparison with carbon fibers. Another choice is basalt fibers. Although they have only recently been developed for civil engineering, the basalt fibers have already demonstrated their mechanical, chemical and economic advantages<sup>13)</sup>. Basalt fibers not only have similar costs and mechanical properties as glass fibers, but they are also much more chemically stable when applied to strengthen structures. In a previous study<sup>14-15)</sup>, basalt FRP were investigated for applications as stay cables to replace CFRP, but results showed that the pure basalt FRP cables would cause low initial stress and large sag in order to maintain equivalent stiffness due to the relatively low modulus. Thus hybridization of basalt and carbon FRP cables was studied and proven to have better integrated performance in terms of static analysis<sup>14-15)</sup>. Based on the previous study, this paper will further discuss the dynamic behavior of cable-stayed bridge with hybrid B/CFRP cables, meanwhile the bridges with steel, CFRP and BFRP cables are also analyzed as references.

## 2. Fundamental properties of stay cables

### 2.1 Mechanical properties

The mechanical properties of the materials available for cables are listed in Table 1.<sup>15)</sup>

Table 1 The mechanical properties

Materials	Density (g/cm <sup>3</sup> )	Elastic modulus (GPa)	Tensile strength (MPa)	Elongation at failure (%)
PC Steel	7.80	195	1770	>3.50
CFRP	1.60	230	3400	1.48
AFRP	1.40	108	1950	1.95
GFRP	2.60	80	1500	1.90
BFRP	2.65	91	2100	2.30
B/CFRP	2.36	130	1949	1.48

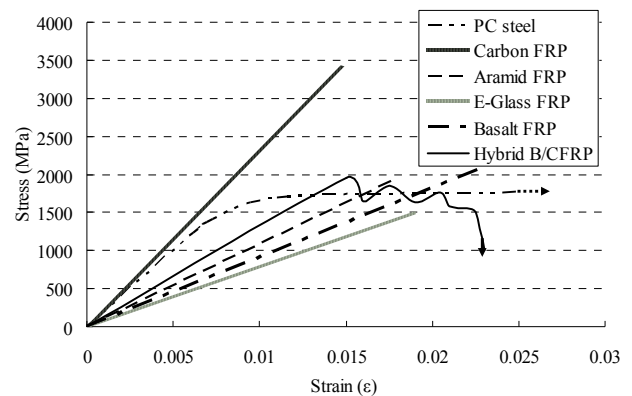


Fig. 1 Idealized stress-strain relationship of different materials

For the convenience of discussion, the mechanical properties of above materials are also plotted in Fig. 1 that shows E-glass, basalt and aramid fibers all exhibit a much lower modulus compared to carbon fibers. Carbon fibers, although possessing a similar initial modulus and better linear stress-strain properties compared with PC steel, are precluded by their high cost from mass use in long-span bridges. Therefore, considering both mechanical and economical requirement, it is reasonable to hybridize carbon and basalt fibers to obtain integrated high performance in both aspects.

### 2.2 Hybrid concept of FRP

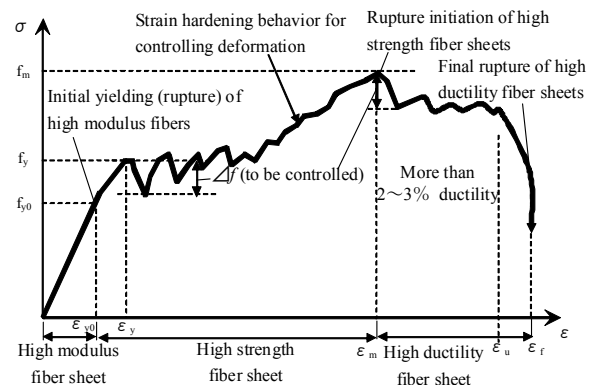


Fig. 2 Idealized stress-strain behavior of hybrid FRP<sup>20)</sup>

In previous studies, the hybrid FRP sheets consisting of high modulus, high strength and high ductility fibers were investigated to strengthen concrete structures<sup>16)</sup>. The high performances of initial stiffness and sufficient ductility have been obtained through tests<sup>17-19)</sup>. Idealized stress-strain behavior of above three kinds of hybrid fiber sheets is shown in Fig. 2, from which, a new kind of hybrid property was obtained by hybridizing three kinds of fibers by controlling the stress drop ( $\Delta f$ )<sup>20)</sup>.

Following this idea, the initial high stiffness and ductility of stay cables can be designed by means of hybridizing high modulus carbon fibers and high ductility basalt fibers. It is also shown in Fig.1 that hybrid B/C fibers with a proportion of 2.57:1 (B:C) exhibit higher stiffness than basalt fibers and linearity before the rupture of carbon fibers, after which the capacity of basalt fibers could continue to be exerted as ductility stock, although this would not be considered in the design of cable. On the one hand, this hybrid method improved the entire material modulus to satisfy the requirement of stiffness; on the other hand, the small amount of carbon fibers would not greatly increase the total cost. Assuming the cost ratio of carbon to basalt fibers is 10, the cost of entire hybrid B/CFRP cables in 1000 m cable-stayed bridge will save 30% in comparison with the CFRP cables. In addition, stress in the cable can still be maintained after the rupture of carbon fibers, which makes the cables safer than carbon fiber cables under some extreme conditions (earthquakes, hurricanes, etc). Therefore, the hybrid proportion of B/C (2.57:1) would be adopted for discussing hybrid B/CFRP cables in static and dynamic analysis. Herein, E-glass fiber will not be considered due to its unstable chemical properties and relatively poor long-term behavior<sup>14-15)</sup>.

### 2.3 Fatigue behavior of FRP

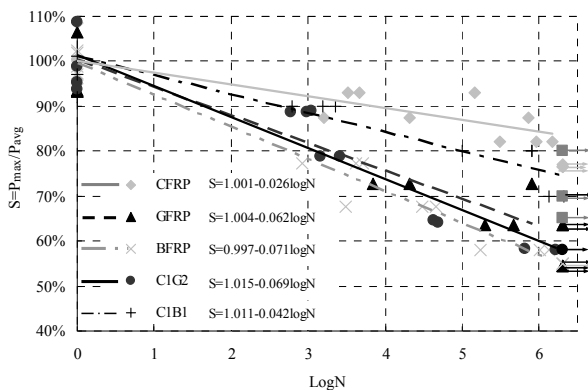


Fig. 3 Fatigue behavior of different FRP composites<sup>21)</sup>

Aside from the short-term mechanical properties of FRP composites described above, the properties related to their long-term behavior such as fatigue resistance are usually considered strictly in the design of stay cables subjected to the dynamic loads. Fatigue tests on CFRP, BFRP, GFRP and hybrid C1B1 (Ratio of C/B=1:1), C1G2 FRP sheets were conducted<sup>21)</sup>.

Test results with S-N curves are shown in Fig.3, which shows that BFRP and GFRP exhibit relatively low fatigue-resistance strength; conversely, the best fatigue resistance behavior can be found in CFRP. Hybridized C1G2 FRP did not show obvious improvements in fatigue resistance, which may be caused by the weak cooperation between carbon and glass fibers. However, the fatigue-resistance strength of hybrid C1B1 FRP was increased significantly and close to the level of CFRP. This hybrid effect on improving fatigue resistance makes hybrid B/C fibers more suitable as stay cables for carrying dynamic loads.

### 2.4 Design of cable section

Following the concept of hybrid B/CFRP cable, the composition of cable section has been studied. Common stay cables usually consist of paralleled wires or strands that are shown in Fig. 4.

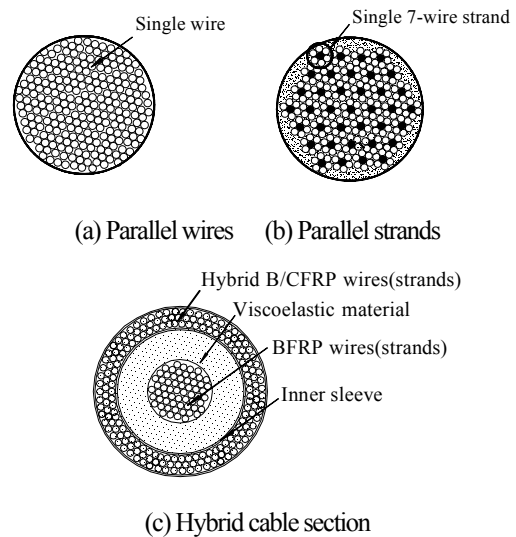


Fig. 4 The composition of wires or strands in the cable

Fig. 4(a) and (b) show that for a single-material cable, like steel, CFRP or BFRP cables, only a parallel arrangement of wires or strands can be adopted to compose the cable. However, for hybrid B/CFRP cables, a special arrangement of wires or strands with considering of aerodynamic stability can be realized due to different properties of two kinds of materials. The hybrid cable section is shown in Fig. 4(c), where each hybrid B/CFRP wire consists of hybridizing carbon fibers and basalt fibers in a certain proportion. In this design, BFRP wires are arrayed in the center of cable, while hybrid B/CFRP wires are arrayed in the outer layers of the cable. The inner sleeve is set for fixing the shape. A gap would be left between the two wires, where a viscoelastic material will be inserted. When the cable is excited by dynamic loads, relative movement between inner BFRP wires and outer hybrid wires may occur due to their inherent differences in sag and vibrational frequency. This relative movement can absorb vibrational energy by compressing the inserted viscoelastic material, which may also be regarded as an enhancement of

inherent damping. Based on this design, the hybrid B/CFRP cables are expected to have superior performance over steel, CFRP, and BFRP in terms of aerodynamic stability. Corresponding research is currently in progress.

### 3. Bridge model and principles

#### 3.1 Parameters of analysis model

Since at present the longest cable-stayed bridge spans 1,088 m, the static analysis models are built according to this size; meanwhile, the models with a main span of 2,176m (twice the size of the existing longest one) are also built to verify the influence of FRP cables with the elongation of span.

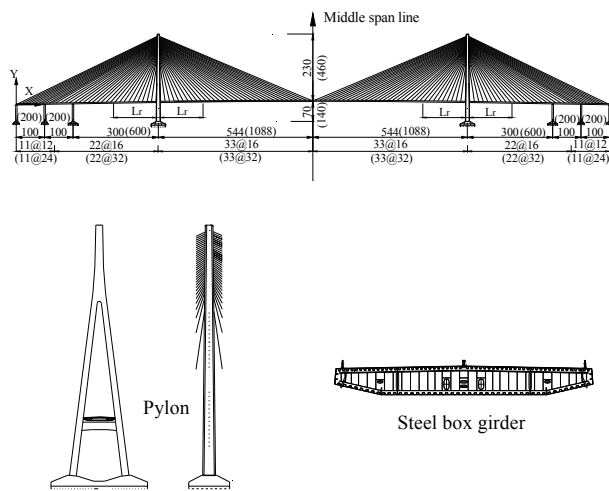


Fig. 5 Elevation of the bridge model (unit: m)

The shape and dimensions of the bridge model are shown in Fig. 5, which are the dimensions of Sutong Bridge<sup>22</sup>. The values in brackets represent the dimensions of the bridge with a 2,176 m span. The main girder is a steel box girder, and pylons and peers are built out of concrete. The reinforced zones of the main girder are denoted as Lr of 168 m (336m for the bridge with 2,176 m span) from the pylon to the two sides. The entire bridge is symmetric with respect to the middle span line. Detailed parameters of the bridge can be found in references<sup>14-15</sup>.

The dead load per unit length ( $F_D$ ) is determined by Eq. (1), which is usually used for calculating the approximate dead load in preliminary design<sup>3</sup>,

$$F_D = 1.4\gamma_s A_s + 70 \quad (\text{kN/m}) \quad (1)$$

where  $\gamma_s$  is the weight density of steel,  $A_s$  is the cross-sectional area of the girder, 1.4 is the coefficient that accounts for the diaphragms, cross beams or other components in the main girder, and 70 kN/m is the superimposed dead load, which accounts for the pavement, handrails, and other attachments. The uniform live load is assumed to be 45 kN/m, with an additional concentrated load of 1,015 kN considered when studying the behavior under the traffic load.

The initial state of the bridge is determined by the principle of minimum moments in the main girder and pylon, which maintains zero displacement at the connection points of the cables and the main girder, and also at the longitudinal direction of the top of the pylon.

#### 3.2 The principle of cable replacement

Two methods are usually adopted to replace steel cables with FRP cables. They are the strength and stiffness principles, which can be expressed by Eq. (2) and (3), respectively.

$$f_d = \frac{f_s}{S} \quad \text{then } A_f = \frac{F_d}{f_d} \quad K_f = E_f A_f \quad (2)$$

$$A_f = \frac{K_s}{E_f} \quad \text{then } f_d = \frac{F_d}{A_f} \quad \text{where } K_s = E_s A_s \quad (3)$$

in Eqs. (2) and (3),  $f_d$  is the design strength of cable,  $f_s$  is the tensile strength of material,  $S$  is the safety factor of material,  $A_f$  is the sectional area of FRP cable,  $F_d$  is the design cable force,  $K_f$  is the stiffness of cable,  $E_f$  is the modulus of FRP cable, and  $K_s$  is the stiffness of steel cable, which can be obtained by multiplying modulus of steel  $E_s$  by sectional area of steel cable  $A_s$ .

In terms of the strength principle, the design strength of CFRP is greater than that of steel due to its much higher tensile strength, and the safety factor is similar to steel, which results in a 74% of the stiffness of steel cable in terms of Eq. (2). For BFRP and hybrid B/C FRP cable, the stiffness only occupies 47% and 74% of the steel cable. The lower of cable stiffness may cause larger middle span deflection under the traffic load, which result in  $1/338 l$ ,  $1/218 l$ ,  $1/338 l$ , respectively for the bridges with CFRP, BFRP and hybrid B/CFRP cables. These deflections not only are larger than that of the steel cables ( $1/463l$ ), but also exceed the deformation restriction ( $1/400l$ ) under the traffic load. Additionally, large deflection would generate extra bending stress in the main girder, which is disadvantageous for the main girder maintaining loads. Therefore, it is not suitable to replace FRP cables with steel cables by means of the strength principle.

Table 2 Design parameters by stiffness equivalent principle

Type of cable	Stiffness	Modulus (GPa)	Sectional area	Design strength (MPa)
Steel	$K_s$	195	$A_s$	708
CFRP	$K_s$	230	$0.85A_s$	835
BFRP	$K_s$	91	$2.14A_s$	330
B/CFRP	$K_s$	130	$1.50A_s$	472

Therefore, the following analysis of FRP cables is based on the stiffness principle, by which the same stiffness of cable can be obtained and the requirement of deflection would be satisfied. As a result, a lower design strength and larger sectional area of FRP cables would be required, especially for the BFRP cables, as shown in Table 2.

### 3.3 Equivalent modulus of different cables

Due to the self-weight of materials, the cable's sag effect would become apparently with the increasing of length that can lead to a low efficiency of material utilization and make the bridge more flexible under traffic load. The steel cables will exhibit obvious sag when the bridge reaches a thousand-meter scale due to its large density. In contrast, the inherently small density of FRP materials, which is only 1/4 to 1/3 of steel, makes them exhibit much smaller sag than steel cable. From the view of stiffness, the increasing sag would make the bridge more flexible so that the actual modulus of the cable could be replaced by the reduced modulus, which is denoted by the Ernst Equation as shown in Eq. (4)<sup>1)</sup>:

$$E_{eq} = \frac{E}{1 + \lambda^2 / 12} \quad \text{where } \lambda^2 = \frac{\gamma_{cb} L^2}{\sigma^3} E \quad (4)$$

where  $E_{eq}$  is the equivalent modulus and  $E$  is the material modulus of the cable.  $\lambda^2$  is a parameter introduced by Irvine and Caughey<sup>23)</sup>, which is widely used in description of stay cables.  $\gamma_{cb}$  is the weight density of cable,  $L$  is the horizontal projected length of cable and  $\sigma$  is the initial stress of cable.

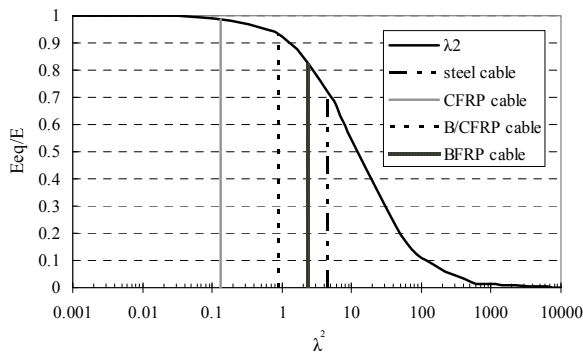


Fig. 6 Equivalent modulus with respect to  $\lambda^2$

The Eq. (4) also can be presented in Fig. 6 that indicates the rate of modulus loss will become apparent when  $\lambda^2$  is larger than 1. The existing bridges close to 1,000 meter span may have a  $\lambda^2$  between 1 and 10, such as the longest cable in Normandy Bridge (856m) with a  $\lambda^2$  of 3.1. The straight lines in Fig. 6 indicate the  $\lambda^2$  of different cables with the length of 1,150 m (for 2,176 m span bridge). For this length, steel and basalt FRP cables only remain 70% and 80% of their initial modulus, whereas CFRP and hybrid B/CFRP cables still maintain 98% and 93% of initial modulus. The equivalent modulus with respect to the increasing of span was shown in Fig. 7. The figure indicates that hybrid FRP cable also achieves superior results, with the equivalent modulus slightly lower than that of the carbon cable but much greater than that of the steel and BFRP cables. In this regard, hybrid B/CFRP cable is also very effective for long-span cable-stayed bridge, and this advantage would be even more pronounced with the elongation of bridge span.

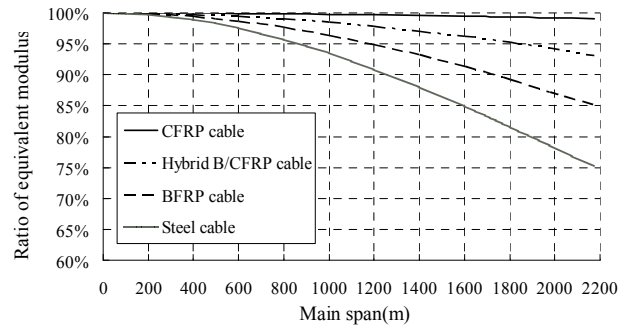


Fig.7 The ratio of equivalent modulus of stay cables

## 4. Dynamic performances of cable-stayed bridge

The entire cable-stayed bridges and stay cables were studied respectively, and their interaction was also addressed. Moreover, the aerodynamic behavior of stay cables is also discussed by the analysis of their Scruton numbers.

### 4.1 Parameters of analysis model

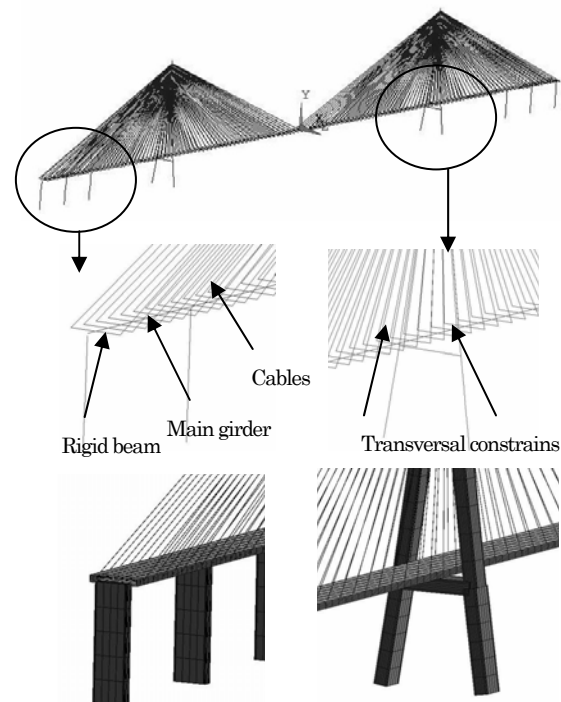


Fig. 8 Dynamic model of cable-stayed bridge (with and without element shapes)

The entire bridges were modelled by the single-beam method. By using this method, the bridge girders, pylon and piers were simulated by three-dimensional beam elements, and the bridge deck was simulated by rigid beams. Between deck and pylon, the cables were simulated by the two-dimensional link elements, as shown in Fig. 8. The sectional properties of the main girder, pylon and piers were modelled through designing sections similar to the real sections. The sag effect of cables was considered by means of defining an equivalent modulus and the initial strain in

the cables was also taken into account. In terms of the above assumptions, the model of the entire bridge was built for dynamic analysis, in which the main girder was connected at the middle-span. The deformations at the connection of piers and main girders were constrained except for longitudinal displacement, and the transverse displacement between the main girder and pylon at the location of the pylon were constrained. The ends of the pylons and piers were fixed.

The model of one single cable was divided by thirty sections to achieve sufficient accuracy, where each section was simulated by two-dimensional beam elements that can automatically calculate sags. The initial strain in the cable was also taken into account due to its contribution to the stiffness of the cable. The two ends of cable were fixed.

## 4.2 Results of analysis

### (1) Dynamic characteristics of the entire bridge

The natural frequencies and the associated mode shapes of the first twentieth modes are presented in Fig. 9 and Table 3.

Table 3 Natural frequencies of bridges with two main spans

Order	Mode shapes	
	1088m span	2176m span
1	Floating	Floating
2	Primary sway	Primary sway
3	Primary heave	Primary heave
4	Secondary heave	Secondary heave
5	Third heave	Third heave
6	Secondary sway	Secondary sway
7	Fourth heave	Fourth heave
8	Tower bending, sym.	Fifth heave
9	Tower bending, anti-sym.	Sixth heave
10	Fifth heave	Tower bending, sym.
11	Sixth heave	Tower bending, anti-sym.
12	Tower secondary bending, sym.	Seventh heave
13	Tower secondary bending, anti-sym.	Eighth heave
14	Seventh heave	Ninth heave
15	Eighth heave	Tenth heave
16	Ninth heave	Tower secondary bending, sym.
17	Tenth heave	Tower secondary bending, anti-sym.
18	Torsion	eleventh heave
19	/	twelfth heave
20	/	Torsion

From Fig. 9, it can be seen that the mode shapes of different bridges at both spans (1,088m and 2,176m) maintain invariance despite the differences in cables, which indicates that the influence of cables to the entire bridge is very small. The natural frequencies of the entire bridge decrease with the increasing of span and the corresponding mode shapes are partially changed, among which torsion mode shape of 2,176 m span bridge appears at the 20<sup>th</sup> order in comparison to the 18<sup>th</sup> of 1,088 m span bridge (Table 3). Because the total masses of stay cables

only occupy a small proportion (approximate 15%) of the bridge main girder, different stay cables with different masses have little influence on the natural frequencies and the corresponding mode shapes of the whole bridges. This result indicates that modal characteristic is only determined by the main girder and pylon of the bridges.

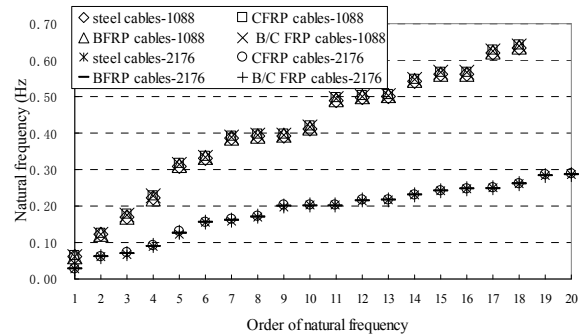


Fig. 9 Natural frequencies of the entire bridge

### (2) Dynamic characteristics of stay cables

Table 4 Natural frequencies of the stay cables with 575 m and 1,150 m

Natural frequency	1,150 m					
	1	2	3	4	5	
Steel	1088m	0.27	0.55	0.82	1.10	1.37
	2,176m	0.14	0.27	0.41	0.55	0.68
CFRP	1088m	0.65	1.31	1.96	2.62	3.27
	2176m	0.33	0.65	0.98	1.31	1.64
BFRP	1088m	0.32	0.63	0.95	1.27	1.58
	2176m	0.16	0.32	0.48	0.64	0.80
Hybrid	1088m	0.41	0.81	1.22	1.63	2.03
	2176m	0.20	0.41	0.61	0.81	1.02

The natural frequencies of the longest stay cables (575 m and 1,150 m) with different materials were calculated, for which the single cable is modelled by two-dimensional beam elements with thirty sections to consider the sag effect. The initial strain in the cable is also taken into account due to its contribution to the stiffness of the cable. The results of the first fifth frequencies are listed in Table 4, and also plotted in Fig. 10.

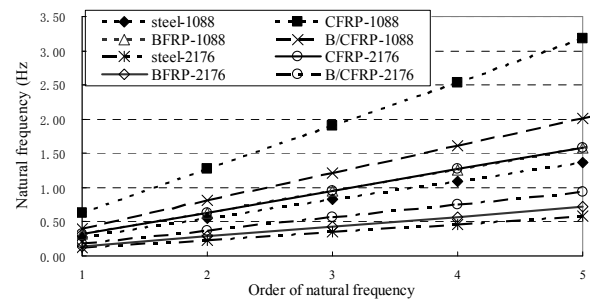


Fig. 10 The first fifth natural frequencies of different stay cables

From Table 4, it can be found that obvious differences in the natural frequencies exist among different cables. CFRP cable exhibits highest natural frequencies in every order due to its low density and small sectional area determined by the equivalent

stiffness principle, whereas the natural frequencies of BFRP cable are very close to those of steel cable, because its weight per unit length is similar to steel cable. Although the natural frequencies of hybrid B/CFRP are lower than that of the CFRP cables, an obvious improvement still can be seen in comparison with steel cables. For 2,176 m span, the natural frequencies of different cables have nearly half of the one with 1,088 m span. This shows linearity of cable's natural frequency with respect to the length. The representation of Table 4 is also plotted in Fig. 10 that can show their variation trend.

### (3) Impact of stay cables to the vibration of bridge

Based on the modal analysis of the entire bridges, the first eighteen and twentieth natural frequencies of 1,088 m and 2,176 m bridges cover the major mode shapes, including floating, sway, heave and torsion. Thus, the possibility of resonance between stay cables and the bridge could be evaluated by comparing these natural frequencies of the bridge and stay cables, which could be conducted from two aspects: one is to compare the first natural frequencies of stay cables that have different lengths with the first eighteen natural frequencies of the bridges; the other is to compare the first few natural frequencies of the longest cables with the first eighteen natural frequencies of the bridges.

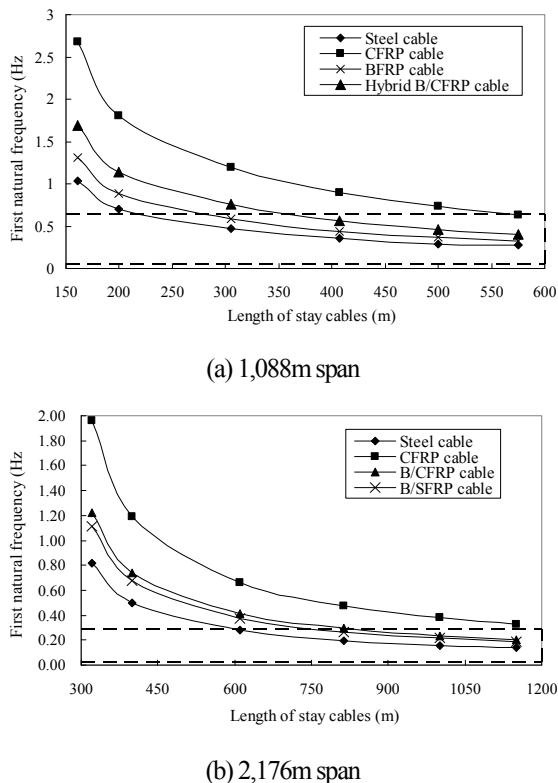


Fig.11 Possibility of resonance between bridges and cables with different lengths

From the first aspect, the actual lengths of the cables (from shortest to longest: 161 m, 202m, 305, 407m, 500 m, and 575m for 1,088m span; 322 m, 404m, 610, 814m, 1,000 m, and

1,150m for 2,176m span) were selected to calculate their first natural frequencies, in which the different sectional areas, the inclined angles, and the initial strains were considered. The analysis results are shown in Fig. 11, where the dashed lines represent the range of the first eighteen (for 1,088m) and twentieth (for 2,176m) natural frequencies of the bridges. It is shown that the majority of steel cables are in the range of possible resonance between the cables and bridge. Obviously, the first natural frequencies of hybrid B/CFRP cables are improved in comparison with steel cables. Thus, a resonance between the cables and bridge will not occur for the cables shorter than 350m, which is 61% of the length of longest cable. And this advantage will become more apparent in 2,176m span bridge, where the resonance will not occur when the cable length below 814m (71% of the length of longest cable). The CFRP cables exhibit the highest first natural frequencies, higher than almost all of the first eighteen/twentieth natural frequencies of the bridge, whereas the natural frequencies of BFRP cables are close to those of the steel, which will exhibit higher possibility of resonance.

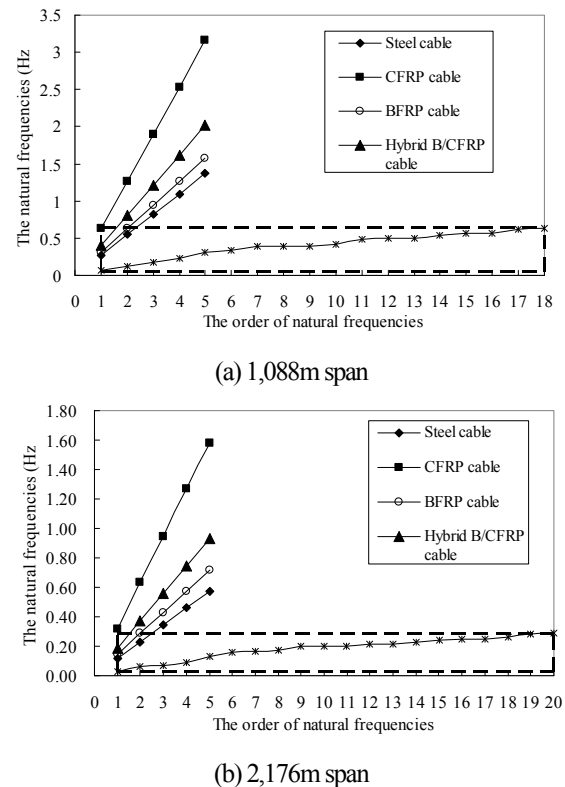


Fig. 12 Possibility of resonance between bridges and cables with different orders

From the other aspect, the first five natural frequencies of different cables with the length of 575m (1,150m for 2,176m span) are adopted to compare the first eighteen/twentieth natural frequencies of the bridge, which is shown in Fig. 12, where the dashed lines also represent the range of the first eighteen/twentieth natural frequencies of the bridge. The figure shows that the first and second natural frequencies of the steel cable and BFRP cable are located in the range of the resonance

risk, whereas only the first natural frequencies of the CFRP cable and hybrid B/CFRP cable are risky of resonance. Little difference could be found between 1,088 m and 2,176 m spans of bridge. Therefore, a lower possibility of resonance can be realized through applying CFRP or hybrid B/CFRP cables. It is proven from above two aspects that the hybrid B/CFRP cables have low possibility of resonance between cables and bridge similarly to CFRP cables, which would benefit the stability of the entire bridge under the vibration.

#### (4) Aerodynamic stability of stay cables

The aerodynamic stability of stay cables is often evaluated by the Scruton number ( $S_c$ )<sup>24</sup>, which is a non-dimensional parameter that represents the occurrence of violent vortex-induced vibrations, as defined by

$$S_c = \frac{2\delta m_e}{\rho D^2} \quad (5)$$

where  $\delta$  is the logarithmic decrement of the cable damping,  $m_e$  is an equivalent mass per unit length,  $\rho$  is the air density, with a value of 1.2 kg/m<sup>3</sup> at 20 °C, and  $D$  is the diameter of the cable.

The cable with a largest sectional area has the smallest  $S_c$  number that means the risk of violent vortex-induced vibrations could be high. Thus, the longest cables with different materials are compared with their  $S_c$  number. The damping coefficient  $\zeta$  ( $\delta \approx \zeta \cdot 2\pi$ ) was set to a value of 0.13% for reference, which is the average measured data from Vasco da Gama bridge<sup>24</sup>. The diameters of the cables consider the actual arrangement of steel wires, while for FRP cables, a 30% proportion of resin to the entire sectional area is assumed when determining the diameters. The comparison is shown in Table 5.

Table 5 The  $S_c$  number of different stay cables

Cables	$m_e$ (kg/m)	$D$ (m)	$S_c$	Decrease (%)	
Steel	575m	65	0.133	50	100%
	1150m	131	0.181	55	100%
CFRP	575m	11	0.144	7	14%
	1150m	22	0.168	11	20%
B/C FRP	575m	30	0.190	11	23%
	1150m	60	0.220	17	31%
BFRP	575m	48	0.230	12	25%
	1150m	96	0.261	19	35%

Table 5 shows that all of the FRP cables exhibit much smaller  $S_c$  compared with the steel cable due to their low densities. It was reported that the risk of violent vortex-induced vibration can be avoided only when  $S_c$  is greater than 20. Moreover, the risk is very significant if  $S_c$  is less than 10<sup>24</sup>. For two kinds of bridge spans, the longest CFRP cables only have  $S_c$  of 7 and 11 that is 14% and 20% of the steel cable. These low  $S_c$  could make them sensitive to vortex-induced vibration. The B/CFRP cables have higher  $S_c$  than the CFRP cables and similar to the BFRP cables. However, it is still insufficient to thoroughly avoid the risk of

violent vortex-induced vibration. The only parameter that could be adjusted to improve the  $S_c$  is the logarithmic decrement of damping, which usually consists of two portions: inherent damping of cable and the damping provided by external damper. Inherent damping of the CFRP cable cannot be improved sufficiently in comparison with the steel cables due to their identical structures. And if installing external dampers to improve the  $S_c$ , the long amount of extra cost would be required. Furthermore, external dampers are usually limited by some architectural requirements.

For the hybrid B/CFRP cable, not only is the  $S_c$  essentially higher than that of the CFRP cable, but also its inherent damping could be designed to achieve a much higher value than the usual steel or CFRP cables by means of separating basalt wires and carbon wires in one cable, as shown in Fig. 4(c). By this method, the vibrational energy could be absorbed through the relative movement of basalt and carbon fiber wires due to their inherent differences in sag and natural frequency. From this perspective, the hybrid FRP cable has more advantages in enhancing the aerodynamic stability. The further theoretical and experimental studies on self-damping behavior of hybrid B/CFRP cables are still in progress.

## 5. Conclusions

The advantages of using hybrid B/CFRP cables in thousand-meter scale cable-stayed bridge were investigated in this paper. Hybrid B/CFRP bridge not only can perform superiorly than steel and BFRP bridges, but also can achieve a high performance similar to CFRP bridge while offering better aerodynamic stability and a low cost. The major conclusions are drawn as follows:

- (1) The major limitations of steel cables in thousand-meter scale cable-stayed bridge lie in a large sag effect and long-term behavior that will make the cables deficient in stiffness and durability. These problems can be overcome by using FRP cables due to their superior mechanical and chemical properties.
- (2) Hybrid B/CFRP can integrate the advantages of both CFRP and BFRP composites, while eliminate their disadvantages simultaneously. This characteristic not only can provide superior mechanical performances for stay cables (relatively high stiffness, small sag, superior fatigue resistance), but also lower the cost and enable practical application of stay cables.
- (3) The 1,088m span bridges with different FRP cables exhibit similar natural frequencies compared with the steel cable bridge, while the mode shapes are constant among the bridges with different cables. The similar rules are observed for 2,176m span bridge. Little influence of different FRP cables on the entire bridge proves that vibrational properties are determined only by bridge girders and pylons instead of

the stay cables.

- (4) The vibrational properties of FRP stay cables differ greatly from the steel one. All of the FRP stay cables exhibit higher natural frequencies than that of steel cables, while CFRP and hybrid B/CFRP cables have much higher natural frequencies than BFRP cables. This characteristic results in a low possibility of resonance between CFRP or hybrid B/CFRP cables and the entire bridge, which manifests more apparently for the cables in 2,176m span bridges.
- (5) Hybrid B/CFRP cables exhibit better aerodynamic stability than the CFRP and BFRP cables due to their adjustable inherent damping. This advantage would greatly enhance the performance for controlling vibration under a dynamic load.

## References

- 1) Gimsing N.J., *Cable supported bridge: concept and design, 2nd edition*, Chichester: John Wiley & Sons, 1997
- 2) Meier U., Proposal for a carbon fiber reinforced composite bridge across the Strait of Gibraltar at its narrowest site, *Proceedings of the Institution of Mechanical Engineers;*, 201(B2), pp.73-78, 1987
- 3) Nagai M., Fujino Y., Yamaguchi H., and Iwasaki E., Feasibility of a 1,400 m span steel cable-stayed bridge, *Journal of Bridge Engineering*, 9(5), pp.444-452, 2004
- 4) Lu Z., Mei K., First application of CFRP cables for a cable-stayed bridge in China, *China Civil Engineering Journal*, 40(1), pp. 50-59, 2007 (in Chinese)
- 5) Cheng S., Lau D. T., Impact of using CFRP cables on the dynamic behavior of cable-stayed bridges, *LABSE REPORTS*, 2006
- 6) Keller T., Recent all-composite and hybrid fiber reinforced polymer bridges and buildings, *Progress in Structural Engineering and Materials*, 3, pp.132-140, 2001
- 7) Keller T., Use of fiber reinforced polymers in bridge construction, *Structural Engineering Documents 7*, Zurich: IABSE-AIPC-IVBH, 2003
- 8) Wu Z., Wang X., and Iwashita K., State-of-the-art of advanced FRP applications in civil infrastructure in Japan, *Composites & Polycon 2007*, American Composites Manufacturers Association, Tampa, FL USA, Oct.17-19, 2007
- 9) Khalifa M. A., Hodhodt O. A. and Zaki M. A., Analysis and design methodology for an FRP cable-stayed pedestrian bridge, *Composites Part B: Engineering*, 27(3), pp.307-317, 1996
- 10) Meier U., Farshad M., Connecting high-performance carbon-fiber-reinforced polymer cables of suspension and cable-stayed bridges through the use of gradient materials, *Journal of Computer-Aided Materials Design*, 3, pp.1-3, 1996
- 11) Noisternig J. F., Carbon fiber composites as stay cables for bridges, *Applied Composite Materials*, 7, pp.2-3, 2000
- 12) Scalea F. L. di, Karbhari V. M., Seible F., The I-5/Gilman advanced technology bridge project, *Proceedings of SPIE*, 3988, pp.10-17, 2000
- 13) Wu Z., Wang X., and Wu G., Basalt FRP composite as a reinforcement in infrastructure (Keynote paper), *The Seventeenth Annual International Conference on Composites/Nano Engineering*, 26 July-1 August 2009, Hawaii, USA (in press)
- 14) Wu Z., Wang X., Investigation on a thousand-meter scale cable-stayed bridge with fiber composite cables, *The Fourth International Conference on FRP Composites in Civil Engineering (CICE-4)*, Zurich, Switzerland July 22-24, 2008(CD-ROM)
- 15) Wang X., Wu Z., Integrated high-performance thousand-metre scale cable-stayed bridge with hybrid FRP cables, *Composites Part B: Engineering*, 2009 (submitted)
- 16) Wu Z., Structural strengthening and integrity with hybrid FRP composites, *Proceedings of the Second International Conference on FRP Composites in Civil Engineering*, Adelaide, Australia, 8-10 Dec. pp.905-912, 2004
- 17) Wu Z., Shao Y., Iwashita K. and Sakamoto K., Strengthening the pre-Loaded RC beams using hybrid carbon sheets, *ASCE Journal of Composites for Construction*; 11(3), pp.299-307, 2007
- 18) Wu, Z., Iwashita, K., Yang, C.Q., Sakamoto, K. and Ahmed, E. Layered hybrid FRP sheets for strengthening structures with integrated performances, *Journal of Reinforced Plastic Composites*, 2008 (In press)
- 19) Wu Z., Wang X., and Iwashita K., Development of high performance structures with hybrid FRP composites, *Proceedings of the 10th International Symposium on Structural Engineering for Young Experts*, Changsha, China, Oct. 19-21, pp.11-20, 2008
- 20) Iwashita, K., Yoshikiyo, K., Wu, Z., Hamaguchi, Y. Experimental study on control index of stress drop for designing hybrid FRP sheets, *Proceedings of 16th International Conference on Composite Materials*, Kyoto, Japan, 2007
- 21) Wu, Z., Wang, X., Iwashita, K., Sasaki, T., and Hamaguchi Y., Tensile fatigue behavior of FRP and hybrid FRP sheets, *Composites Science and Technology*, 2009 (submitted).
- 22) Zhang X., General design of Sutong bridge, *Highway 7*, pp.1-11, 2004 (in Chinese)
- 23) Irvine H. M., Caughey T. K., The linear theory of free vibrations of a suspended cable, *Proceedings of the Royal Society of London, Series A*, Vol. 341, pp.299-315, 1974
- 24) Caetano E. de Sa, Cable Vibrations in Cable-stayed Bridges, *Structural Engineering Documents 9*, Zurich: IABSE-AIPC-IVBH, 2007

(Received: April 9, 2009)